Scientific Research and Essays Vol. 7(15), pp. 1592-1604, 23 April, 2012
Available online at http://www.academicjournals.org/SRE
DOI: 10.5897/SRE12.065
ISSN 1992-2248 ©2012 Academic Journals

Full Length Research Paper

Synthesis and Characterization of Al, Cu, Zn, Mg-Kapok carbon fiber composites

Wanvilai Singse, Sumrit Mopoung* and Anchalee Sirikulkajorn

Department of Chemistry, Faculty of Science, Naresuan University, Thailand.

Accepted 5 April, 2012

This research was conducted to characterize the properties of the metal–carbon fiber composites. The metal-carbon fibers composites were synthesized from the metal salt of Al or Cu or Zn or Mg and kapok fiber by pyrolysis at 400 to 700°C. The composites products were characterized by FTIR, XRD, SEM and EDS. Generally, it was found that the crystalline of all metal-carbon composites have been reduced as the pyrolysis temperature increases from 400 to 700°C. The composites of all kind have a tendency of a decreasing percent yield with increasing temperature of pyrolysis from 400 to 700°C. The oxidizing strength of metal salts are arranged in order Al_2O_3 < $ZnCl_2$ < $MgSO_4.7H_2O$ < $Cu(NO_3)_2$. The amount of metal-carbon composite on surface of kapok carbon fiber was ordered as follows: Zn-carbon composite < Cu-carbon composite < Mg-carbon composite < Al-carbon composite.

Key words: Kapok, carbon fiber, metal-carbon fiber composite, pyrolysis.

INTRODUCTION

Carbon nanotubes have amazing electronic and mechanical properties which lead to incredible forms of strength, and conductivity. From reinforcements in composites, sensors and probes, energy storage, electrochemical devices and nanometer sized electronics carbon nanotubes could revolutionize the world (Paradise and Goswami, 2007). The other application is using as high-capacity hydrogen storage media (Popov, 2004). Currently, state-of-the-art nano-technological techniques such as thin-firm fabrications by sputtering or composite formations by ball milling have been applied to develop new high-performance H-storage materials composed of light elements all over the world. Especially, the pathways to design the mixing between some complex hydrides and/or metal hydrides by the ball-milling method have been studied by Fujii and Ichikawa (2006).

Incorporation of silver metal catalyst into carbon nanotubes increases the hydrogen storage capacity up to 0.86 wt% which is approximately 40% more as compared To purified carbon nanotubes measured under similar experimental conditions. Enhancement of hydrogen storage capacity in Ag/CNT hybrid is due to the spillover of physisorbed hydrogen by metal catalyst onto the carbon nanotubes (Rather et al., 2008). Carbon composites obtained from Mg and carbon black, graphite and carbon nanotube can store hydrogen 5 wt%. Especially, the Mg-graphite composite can store hydrogen up to wt% and discharge wt% at °C (Huang et al., 2007). The hydrogen storage in Mg-graphite composite powder is higher than pure graphite and discharged at 395°C (Imamura et al., 2002). It was also found that the Mg–23.5 wt% Ni and 2 wt% CNTs composite can absorb hydrogen up to 6.1 wt% Schaller et al., 2009). Ndungu et al. (2008) have found that a mixture of carbon nanotubes (CNTs) and Mg and or Pd powder absorbed hydrogen at more than 3.0 wt%. It was also found that Mg-5 wt% MWNTs (multi-walled nanotubes) composite can absorb hydrogen up to 5.34, 5.89 and 6.08 wt% at 100, 200 and 280°C, respectively (Chena et al., 2004). Similarly, the MgH_2/5 wt% SWNTs (single walled nanotubes) composite ground for 10 h absorb hydrogen up to 6.7 wt% and discharge hydrogen of 6 wt% within 5 min at °C (Wu et al., 2006)

This research was conducted to characterize the

*Corresponding author. E-mail: sumritm@nu.ac.th.

Table 1 Percent yield of metal-carbon fiber composites by pyrolysis at 400 to 700°C.

Composite types	% yield of composites by pyrolysis at			
	400°C	500°C	600°C	700°C
Al-kapok carbon fiber composite	71.87	65.56	70.94	66.10
Cu-kapok carbon fiber composite	25.31	24.73	24.33	24.03
Mg-kapok carbon fiber composite	46.16	43.32	40.03	20.65
Zn-kapok carbon fiber composite	71.57	58.69	58.59	47.72

chemical structure, crystalline, surface morphologies and composition of the metal–carbon fiber composites. The metal-carbon fibers composites were synthesized form the metal salt of Al or Cu or Zn or Mg and kapok fiber by pyrolysis at 400 to 700°C. The effects of metal salts and pyrolysis temperature on the formation of the metal–carbon fiber composites were investigated by FTIR, XRD, SEM and EDS. FTIR (Fourier transform infrared spectroscopy) and EDS (Energy Dispersive X-Ray Spectrometer) were used to determine the chemical structure and composition of the metal–carbon fiber composites. SEM (Scanning Electron Microscope) was used to observe surface morphologies. The XRD (X-ray diffractrometer) was studied to inspect the crystalline properties of metal–carbon fiber composites. The composites may be used as a potential hydrogen storage material.

MATERIALS AND METHODS

The kapok fiber (a silky plant fiber that clothes the seeds of the plant species *Ceiba pentandra*. (Lim and Huang, 2007), obtained from agricultural farm in Phitsanulok, Thailand) was dried in the oven (SL 1375 SHEL LAB 1375 FX) at 105°C for h. The fixed carbon, ash content and volatile matter content of kapok fiber were analyzed by methods of ASTM D 3172-89 (1994), ASTM D 2866 – 94 (1996) and ASTM D 5832 – 95 (1996), respectively. Fibers were treated using 5%wt metal salt (aluminiumoxide; Al_2O_3 or copper nitrate; $Cu(NO_3)_2$ or zinc chloride; $ZnCl_2$ or magnesium sulfate; $MgSO_4.7H_2O$). The mixed samples were pyrolysed in closed crucible at 400, 500, 600, and 700°C for 1 h using an electric furnace (Fisher Scientific Isotemp ® Muffle furnace). Pyrolysis was performed at a rate of 10°C/min, a holding time of 1 h at each the needed final temperature value (400, 500, 600, and 700°C) and a cooling rate of 20°C/min. The percent yield of pyrolysed products was calculated. The metal-carbon fiber composites were characterized using FTIR Perkin Elmer, FT-IR System Spectrum GX), XRD (PW 3040/60, X' Pert Pro MPD), SEM and EDS (LEO 1455 VP electron microscopy).

RESULTS AND DISCUSSION

Approximated analysis of the fixed carbon, volatile matter, and ash content of the kapok fiber are 42.38, 55.16, and 2.46%, respectively. The kapok fiber in this study showed that ash content is relatively high as compared to the study by Lim and Huang (2007). Lim and Huang (2007) have found that the ash content of the kapok fiber is only 0.78%. Because of raw kapok fiber in this study is natural product that has not yet got rid of dust. Kapok has a relatively high content of volatile material, such as cellulose, wax, carbohydrate or polysaccharide, lignin, and lignocellulosic (Lim and Huang, 2007). As kapok fiber is pyrolysed, the functional groups of compounds in kapok fiber are removed by thermal decomposition reaction.

In the reduction condition, compounds containing carbon as a main component of the kapok fiber has been reduced to carbon, which is consistent with the fixed carbon content. The high fixed carbon content of the kapok fiber is considered to be the production of carbon fiber.

From Table 1, it can be seen that composites of all kind have a tendency of a decreasing percent yield with increasing temperature of pyrolysis from 400 to 700°C. However, it was found that the Al-kapok carbon fiber composite showed a different pattern. The percent yield of the Al-kapok carbon fiber composite decreased from 71.87 to 65.56% as pyrolysis from 400 to 500°C. After that, it increased to 70.94% at 600°C, which is close to the value at 400°C. But, it remained 66.10% at 700°C, which is slightly higher than the value at 500°C. Xu et al. (2011) have been explained that it was related to the strongly chemisorbed CO_2. The conversions of CO_2 are strongly depended on reaction temperature ranges of 650 to 800°C. The Al_2O_3 composite oxides are highest catalytic activity at 650-800°C due to the intensely endothermic character. The percent yield of the Cu-kapok carbon fiber composite remained relatively constant as the pyrolysis temperature increased from 400 to 700°C (in the range of 25.31 to 24.03%). For Mg-kapok carbon fiber composite the percent yield fell gradually from 400 to 600°C (46.16 to 40.03%) and decreased rapidly at 700°C (with only 20.65%). Finally, in Zn-kapok carbon fiber composite the percent yield was relatively high at 400 °C (71.57%), while it was almost constant (58.89 to 58.59%) at 500 to 600°C and declined moderately (only 47.72%) at 700°C. The decomposition reaction of kapok fiber depends on the type of metal salt. The decomposition strength of metal salts to kapok fiber is in the order $Al_2O_3 < ZnCl_2 < MgSO_4.7H_2O < Cu(NO_3)_2$. This sequence is expected to comply with the oxidizing

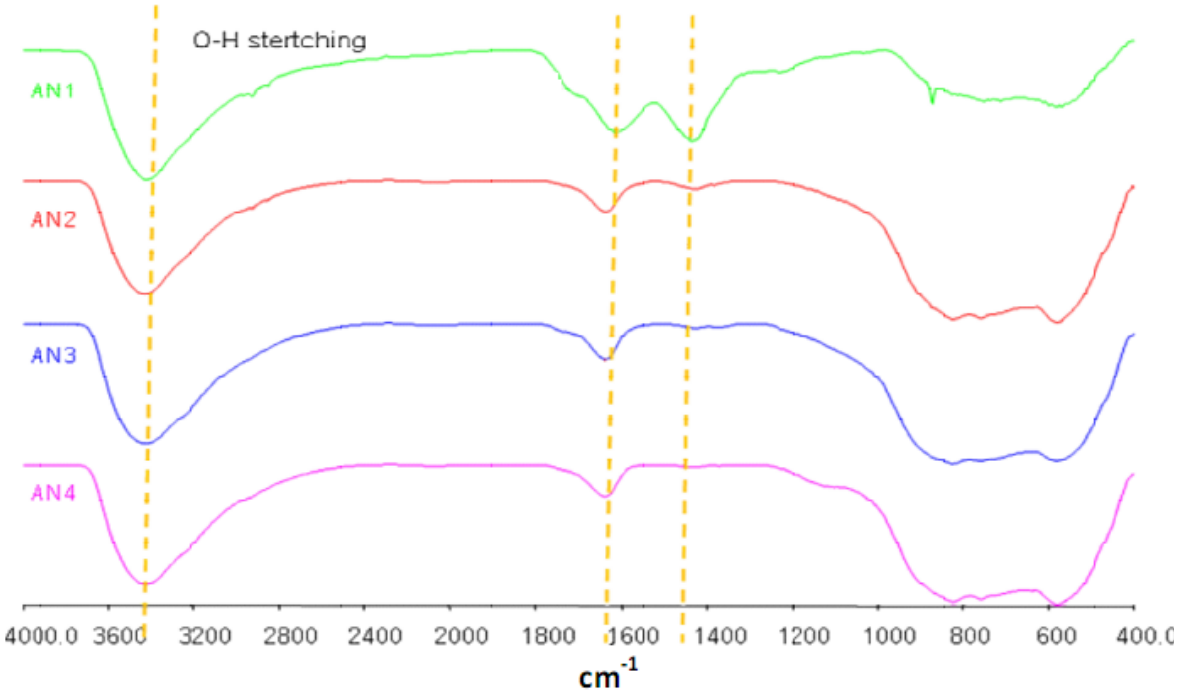

Figure 1. FTIR transmission spectra of aluminium-kapok carbon fiber composites by pyrolysis at 400 to 700°C: AN1 = aluminium-kapok carbon fiber composite at 400°C, AN2 = aluminum-kapok carbon fiber composite at 500°C, AN3 = aluminium-kapok carbon fiber composite at 600°C, and AN4 = aluminium-kapok carbon fiber composite at 700°C.

strength of metal salts.

FTIR analysis

The FT-IR spectra of Al-kapok carbon fiber composite are shown in Figure 1. All composites displayed the following bands: the broad band at 3435 cm^{-1} and weak band at 1639 cm^{-1}. Both bands are due to the vibrations of O–H groups in stretching and bending, respectively (Chłopek et al., 2008). Additionally, the broad and weak bands in the range of 823 to 582 cm^{-1} for all temperatures of pyrolysis are attributed to C–H bending (Oh et al., 2005). Only the Al-kapok carbon fiber composite, which was pyrolysed at 400°C, showed a weak band with very little of the HCH and OCH in-plane bending vibrations at 1435.98 cm^{-1} (Oh et al., 2005). This band disappeared after pyrolysis up to 500°C. The band at 1435.98 cm^{-1} decreased and eventually disappeared with increasing temperature from 400 to 700°C, whereas the band at 823 cm^{-1} showed a remarkable increase. The first band is designated as a crystalline and the second one as an amorphous transmission band. The transmittance intensities at 823 and 1430 cm^{-1} are also very sensitive to the amount of crystalline versus amorphous structure of carbon, that is, broadening of these bands reflects higher amount of disordered structure (Oh et al., 2005).

In Figure 2, FTIR spectra of the Cu-kapok carbon fiber composites show peaks that are weaker than the Al-kapok carbon fiber composites. However, there are broad and weak peaks at 3436 cm^{-1} (O–H group stretching) and very weak peaks at 1639 cm^{-1} (O–H group bending) in all spectra, which indicates that H-bonding has almost been destroyed. Similarly, a very weak peak at 1436 cm^{-1} exists, which almost disappears at temperatures above 600°C. This phenomenon indicates that the HCH and OCH groups have been broken. However, the peak at 823 cm^{-1} does not appear as well.

The conclusion is that the products are more crystalline. Similarly, a relatively strong and sharp peak at 535 cm^{-1} (C–C stretching vibrations) can be seen in all of the spectra.

In Figure 3, FTIR spectra of the Mg-kapok carbon fiber composites show broad and weak peaks at about 3400 cm^{-1} (O–H group stretching) and very weak peaks at 1655 cm^{-1}. The peak at 1655 cm^{-1} gradually decreases with increasing temperature from 400 to 700°C. The FTIR spectrum at 400°C has a peak at 1087.50 cm^{-1} (C-O stretching), which is weaker for higher temperatures in the range from 500°C to 700°C. The FTIR spectrum at 700°C has weak peaks at 1655 and 1111.59 cm^{-1} (C-O or C-O-C stretching vibrations) (Pamuła et al., 2001), 520 cm^{-1} (C–C stretching vibrations). The FTIR spectra at 500 to 600°C show peaks at 1178 cm^{-1} (C-O stretching

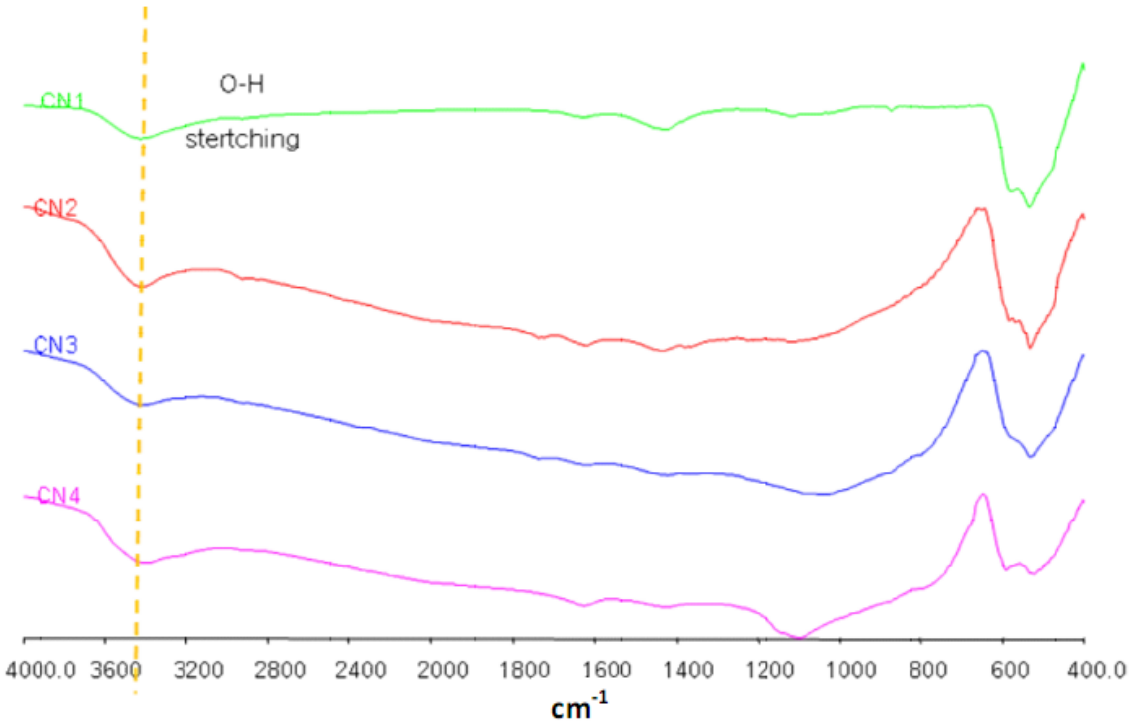

Figure 2. FTIR transmission spectra of copper-kapok carbon fiber composite by pyrolysis at 400 to 700°C: CN1 = copper-kapok carbon fiber composite at 400°C, CN2 = copper-kapok carbon fiber composite at 500°C, CN3 = copper-kapok carbon fiber composite at 600°C, and CN4 = copper-kapok carbon fiber composite at 700°C.

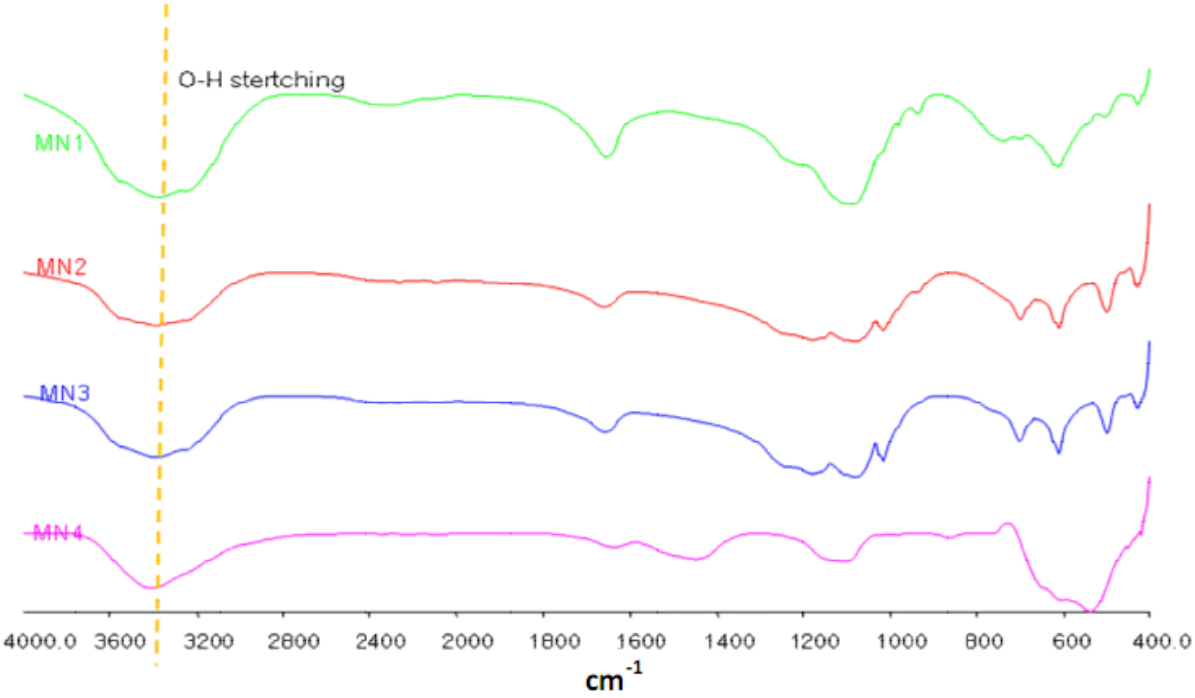

Figure 3. FTIR transmission spectra of magnesium-kapok carbon fiber composites by pyrolysis at 400 to 700°C: MN1 = magnesium-kapok carbon fiber composite 400°C, MN2 = magnesium-kapok carbon fiber composite at 500°C, MN3 = magnesium-kapok carbon fiber composite at 600°C, and MN4 = magnesium-kapok carbon fiber composite at 700°C.

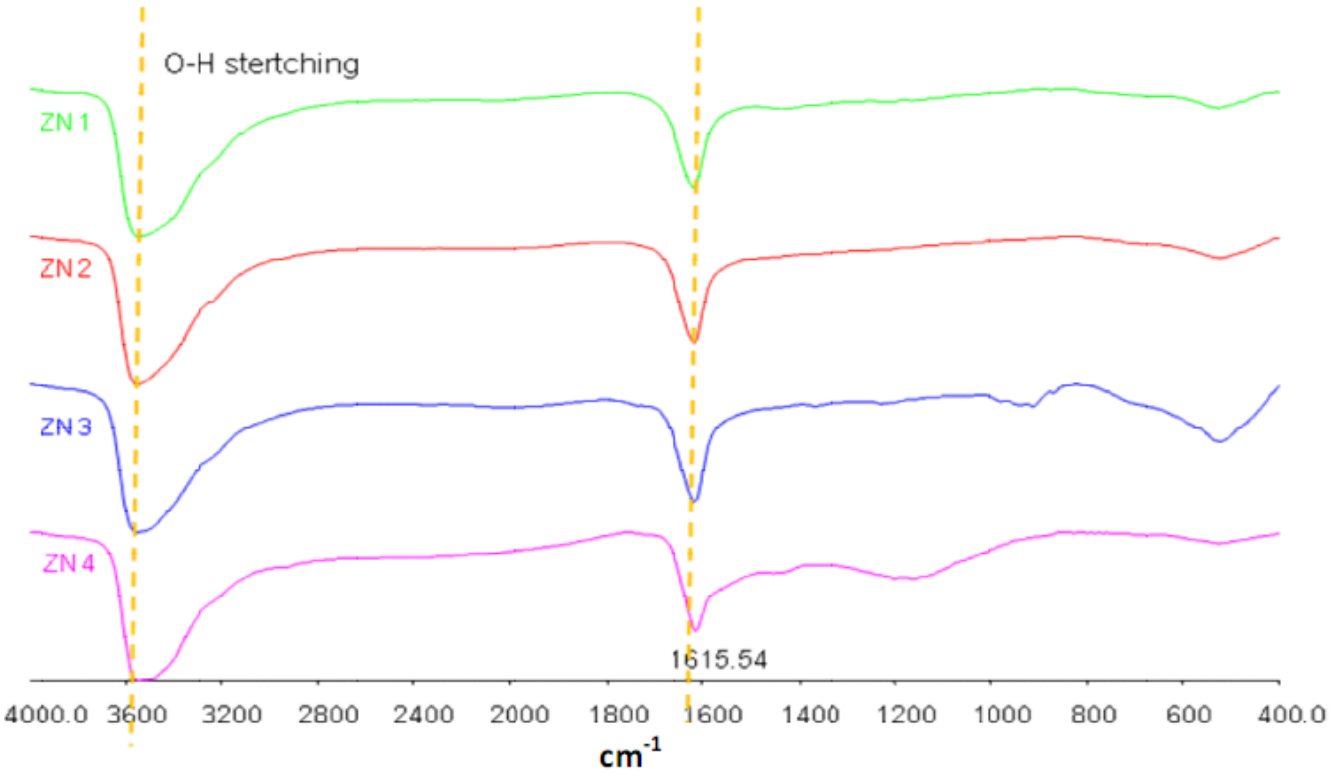

Figure 4. FTIR transmission spectra of zinc-kapok carbon fiber composites by pyrolysis at 400 to 700°C: ZN1 = zinc-kapok carbon fiber composite at 400°C, ZN2 = zinc-kapok carbon fiber composite at 500°C, ZN3 = zinc-kapok carbon fiber composite at 600°C, and ZN4 = zinc-kapok carbon fiber composite at 700°C.

vibrations) and range from 700 to 498 cm^{-1} (C–C stretching vibrations) (Chłopek et al., 2008). Similarly, FTIR spectra of the product at 400 to 600°C show peaks at 612 and 429 cm^{-1} which corresponds to the C-C stretching vibrations (Chłopek et al., 2008). The results of FTIR show that with increasing pyrolysis temperature the amount of H-bonding decreases. However, the strength of the H-bonding strength increases to near ideal bonding on the basis of a relatively sharp peak at 3400 cm^{-1} and a weak peak at 1655 cm^{-1}, respectively. The spectrum at 700°C (Figure 3 MN4) shows peak at 1451 cm^{-1} which correspond to the C = O group. This C = O group has been formed by the oxidation reaction.

In addition, the spectrum also shows a crystalline product which may be due to a high amount of Mg compound, while C is degraded to a large number (Table 1). In addition, the intensity of the peak at 1087.50 cm^{-1}, which corresponds to CO stretching, decreases when the temperature increases from 400 to 700°C. This result indicates a thermal decomposition of functional groups.

Figure 4 shows the FTIR spectra of Zn-kapok carbon fiber composites. There is a relatively sharp peak at 3560 cm^{-1}, a narrow peak at 1618 cm^{-1} and a very weak peak at 525 cm^{-1} (C–C stretching vibrations)(Chłopek et al., 2008). The maximum transmittance of hydrogen-bonded OH stretching (3560 cm^{-1}) is shifted to higher wavenumber as compared to other metals. The OH bending mode is also shifted to lower wavenumber (1618 cm^{-1}). The OH stretching is mainly due to intramolecular hydrogen bonding with increased by Zn. The FTIR spectrum of the product at 700°C (Figure 4 ZN4) has a broad peak at 1100-1200 cm^{-1}, which corresponds to the stretching C-O group vibrations of polyester bonds (Pamuła et al., 2001). This shows that oxidation has occurred at this temperature. In addition, the intensity of the peaks in the range 500 to 800 cm^{-1} is very small (less C-C stretching vibration). It concludes that the products are amorphous.

Comparative effects of different metals-carbon fiber composites pyrolyzed at different temperature were found that the FTIR spectra showed increasing of amorphous structure of all metals-composites as pyrolysis temperature increased. The FTIR spectra of all Cu-kapok carbon fiber composites showed minimal intensity of peaks. It showed that the functional groups were good degraded by Cu-salt. The peaks of OH stretching of all metals-composites are trend to narrowing with shifted to higher wavenumber as pyrolysis temperature increased. This phenomenon was most evident in Zn-kapok carbon fiber composites. The intensity of OH peaks is relatively stable in Al-kapok carbon fiber composites for all pyrolysis temperature. The

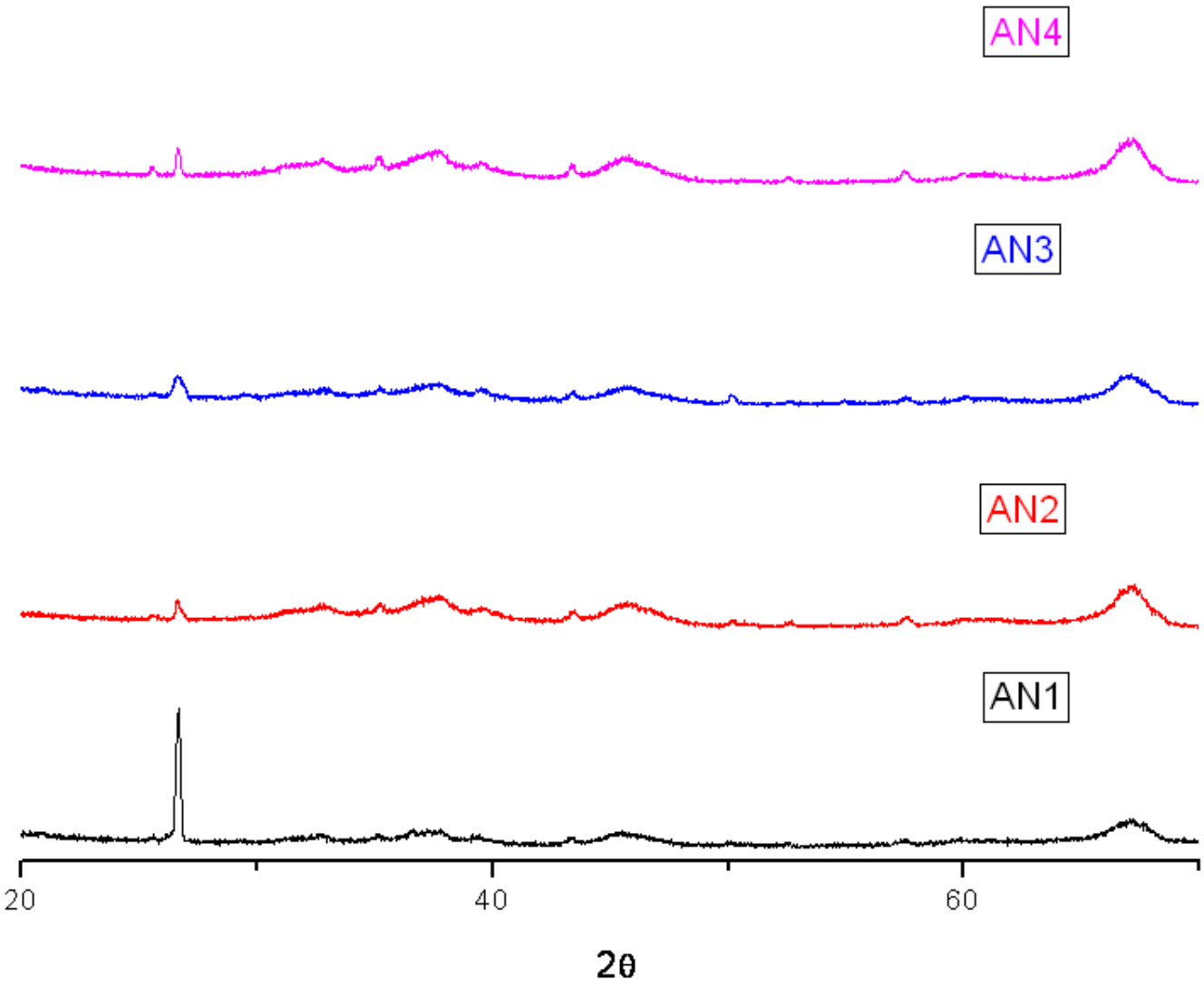

Figure 5. X-ray powder diffraction spectra of aluminium-kapok carbon fiber composites by pyrolysis at 400 to 700°C: AN1 = aluminium- kapok carbon fiber composite at 400°C, AN2 = aluminium-kapok carbon fiber composite at 500°C, AN3 = aluminium-kapok carbon fiber composite at 600°C, and AN4 = aluminium-kapok carbon fiber composite at 700°C.

intensity of other peaks (e.g. C=O, C-H, C-C) of all metals-composites is decreased with increasing of pyrolysis temperature.

XRD analysis

The XRD spectra of the aluminium-kapok carbon fiber composites (Figure 5) show a peak performance at 26.5°, which is characteristic of graphite (Eswaramoorthi et al., 2006). The intensity of this peak is reduced above 500°C. At the same time, there is a broad peak at 46°, which is characteristic of amorphous carbon (Fan et al., 2011). Also, broad peaks at about 38° and 68° can be seen, which indicate poorly crystallized Al_2O_3 (Birjega et al., 2009). The results of XRD are consistent with the FTIR spectra (Figure 1).

Figure 6 is the XRD of copper-kapok carbon fiber composite with the dominant peak at about 36° and 39° in all spectra, which indicates the characteristics of CuO (Eswaramoorthi et al., 2006). This is consistent with the results of percent yield of the products after pyrolysis at temperatures ranging from 400 to 700°C. It was shown that the oxidizing power of CuO is very high. The effect of CuO oxidation has resulted in an increased amount of Cu in the composition of the material. In addition, these spectra also show that the pyrolysis product is crystalline. This is consistent with the results of FTIR (Figure 2). Finally, the peak of the carbon fiber is a weak peak at about 26.5° for all spectra that it is amorphous

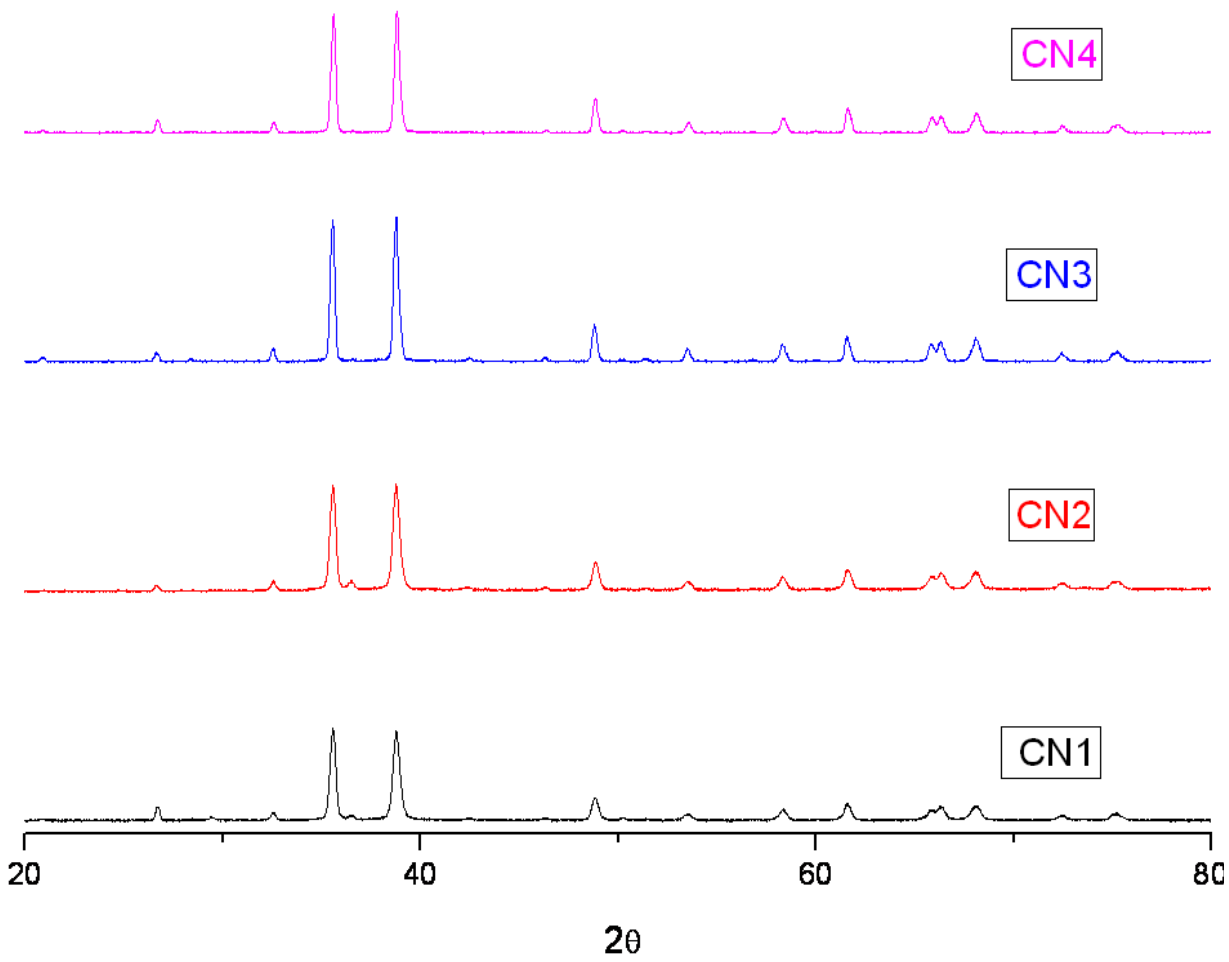

Figure 6. X-ray powder diffraction spectra of copper-kapok carbon fiber composite by pyrolysis at 400 to 700°C: CN1 = copper-kapok carbon fiber composite at 400°C, CN2 = copper-kapok carbon fiber composite at 500°C, CN3 = copper-kapok carbon fiber composite 600°C, and CN4 = copper-kapok carbon fiber composite at 700°C.

(Eswaramoorthi et al., 2006).

Figure 7 shows XRD spectra of magnesium-kapok carbon fiber composites. It was found that the composites with pyrolysis at 400 to 600°C are amorphous. In contrast, peaks in the spectrum at 700°C indicate a crystalline product of pyrolysis, which is consistent with the dominant FTIR peak at 1451 cm^{-1}, while the peak at 823 cm^{-1} is very weak.

XRD spectra of the zinc-kapok carbon fiber composites are shown in Figure 8. The crystalline content of the composite increases with increasing temperatures from 400 to 600°C. The composite is quite amorphous at 700°C. This is consistent with FTIR data (Figure 4 ZN4), which show that there are C = O groups. This phenomenon has been shown that oxidized carbon fiber is enormous. As a result, the crystal structure is destroyed. All spectra have a peak at about 11° due to the presence of nanoscale particles in the composite carbon fiber (Park et al., 2003). Two peaks of spectra at about 26° and 44° are corresponding to graphite (Eswaramoorthi et al., 2006). Other peaks, the weak peaks at about 32°, 38° and 58° are the peaks of the Zn compound (Wang et al., 2010).

SEM analysis

The kapok carbon fiber has a hollow tubular structure as shown in Figure 9, with an external diameter of 17.98 μm, which is consistent with the study of Lim and Huang (2007). Upon addition of 5 wt% Al_2O_3 into the kapok carbon fiber then pyrolysis at 400 to 700°C, the product has been shown that a large number of particles adhered on the surface of kapok carbon fiber. In contrast, the pyrolysed product at 700°C shows only a few particles (Figure 9 AN1-AN4). Kapok carbon fiber is bent and a groove on the surface. As the pyrolysis temperature increased from 500 to 700°C, it was found that the fracture of carbon fiber increased. This indicates that the temperature had affected the characteristics of

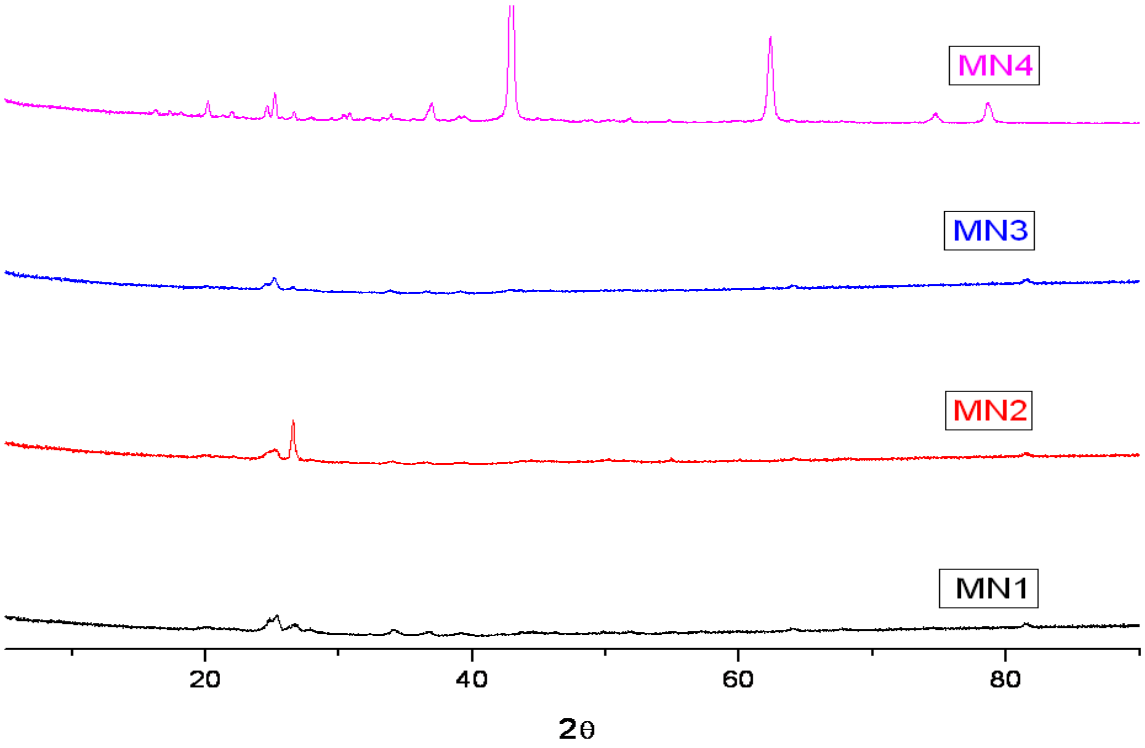

Figure 7. X-ray powder diffraction spectra of magnesium-kapok carbon fiber composites by pyrolysis at 400 to 700°C: MN1 = magnesium-kapok carbon fiber composite 400°C, MN2 = magnesium-kapok carbon fiber composite at 500°C, MN3 = magnesium-kapok carbon fiber composite at 600°C, and MN4 = magnesium-kapok carbon fiber composite at 700°C.

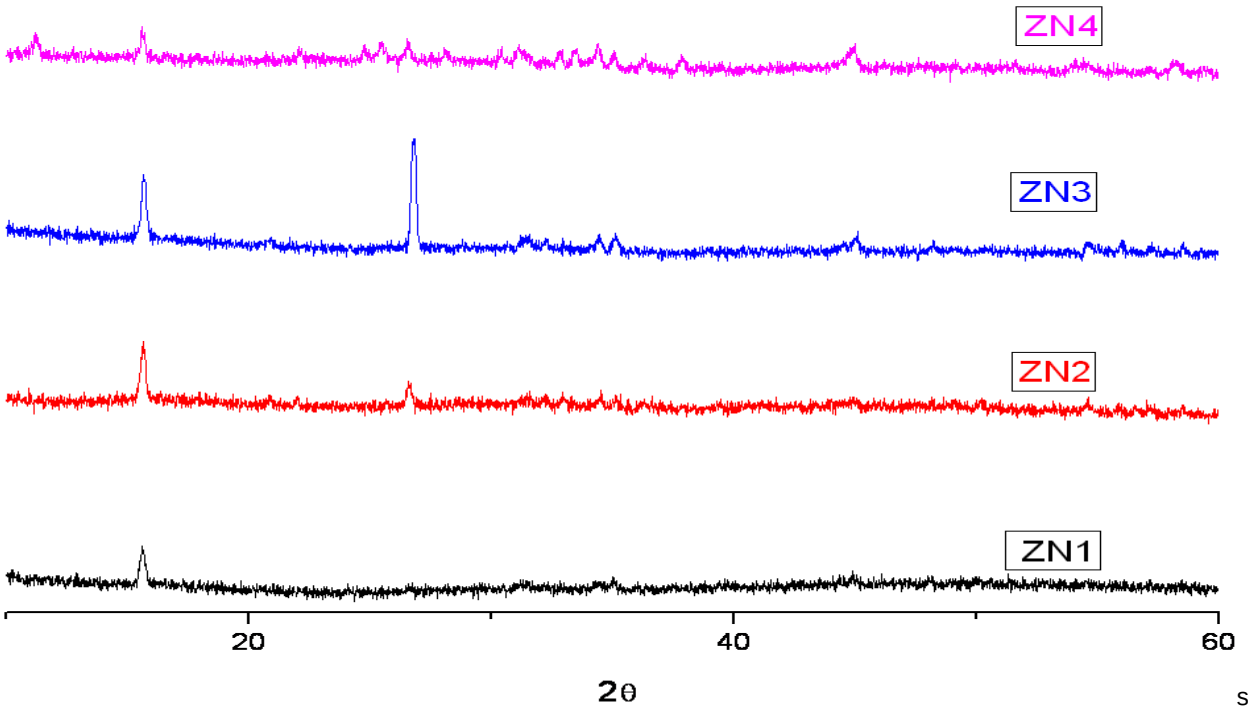

Figure 8. X-ray powder diffraction spectra of zinc-kapok carbon fiber composites by pyrolysis at 400 to 700°C: ZN1 = zinc-kapok carbon fiber composite at 400°C, ZN2 = zinc-kapok carbon fiber composite at 500°C, ZN3 = zinc-kapok carbon fiber composite at 600°C, and ZN4 = zinc-kapok carbon fiber composite at 700°C.

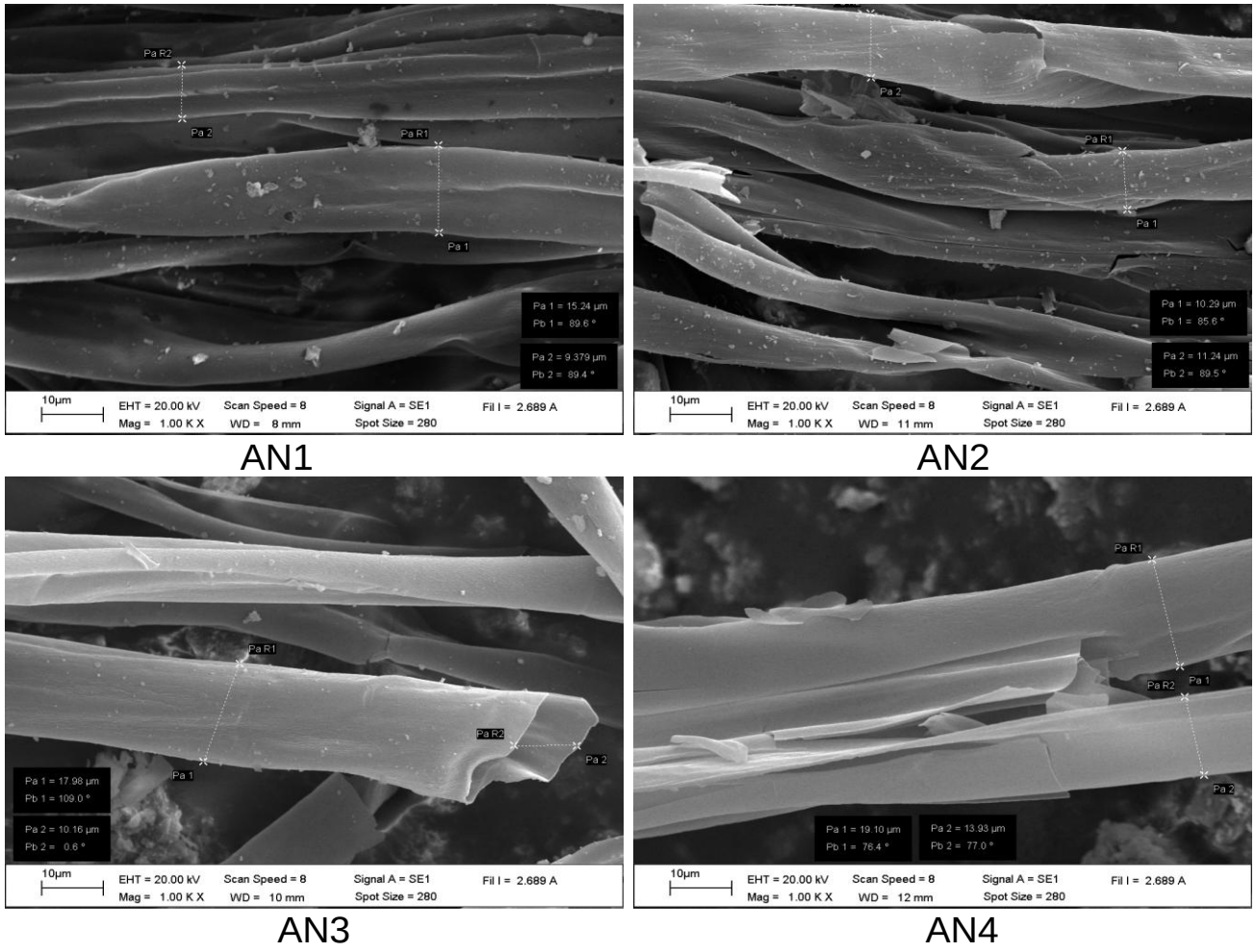

Figure 9. SEM micrographs of aluminium-kapok carbon fiber composites by pyrolysis at 400 to 700°C: AN1 = aluminium-kapok carbon fiber composite at 400°C, AN2 = aluminium-kapok carbon fiber composite at 500°C, AN3 = aluminium-kapok carbon fiber composite at 600°C, and AN4 = aluminium-kapok carbon fiber composite at 700°C.

carbon fiber. Consistent with the XRD data, it was found that the crystallinity reduces as the pyrolysis temperature increases.

SEM images of copper-kapok carbon fiber composites are shown in Figure 10. The surface of kapok carbon fibers are bent and collapsed. However, the SEM thermograph of copper-kapok carbon fiber composites (Figure 10) shows higher convoluted kapok carbonfibres than for aluminium-kapok carbon fiber composite. However, the surface of the copper-kapok carbon fiber composite showed more smooth cylindrical surfaces. The effect of the Cu salt to break the kapok fiber is stronger than the Al salt. In particular, the high-temperature pyrolysis is consistent with the percent yield (Table 1). The percent yield of copper-kapok carbon fiber composite is very low. Consistent with the results of FTIR (Figure 2), the spectrum has a relatively smooth peak. It was confirmed that there are very few functional groups. Based on the results of XRD (Figure 6), it was found that the peak of Cu is very high. This is consistent with the EDS spectrum (Figure 13), where the Cu content is found to be up to 40.98 wt%.

In Figure 11, SEM images of Mg-kapok carbon fiber composite show the effect of Mg on the kapok carbon fiber pyrolysis in the range of temperature pyrolysis between 400 to 700°C. It was found that the particles are trapped on the surface of carbon fiber, which is expected for Mg-carbon composites. At temperatures above 600°C (Figure 11 MN3 - MN4), the collapse and crevices of carbon fibers occurred. Moreover, at 700°C (Figure 11 MN4), there are a high number of particles on the surface of carbon fiber. From this phenomenon, it is clear that the fiber had been significantly degraded. This is consistent with the percent yield (Table 1), where the percent yield of Mg-carbon fiber at 700°C is only 20.65%. It is also consistent with the results of XRD (Figure 7 MN4), and shows prominent peaks associated with Mg. From Figure 3 MN4, the FTIR results also showed that the peak is

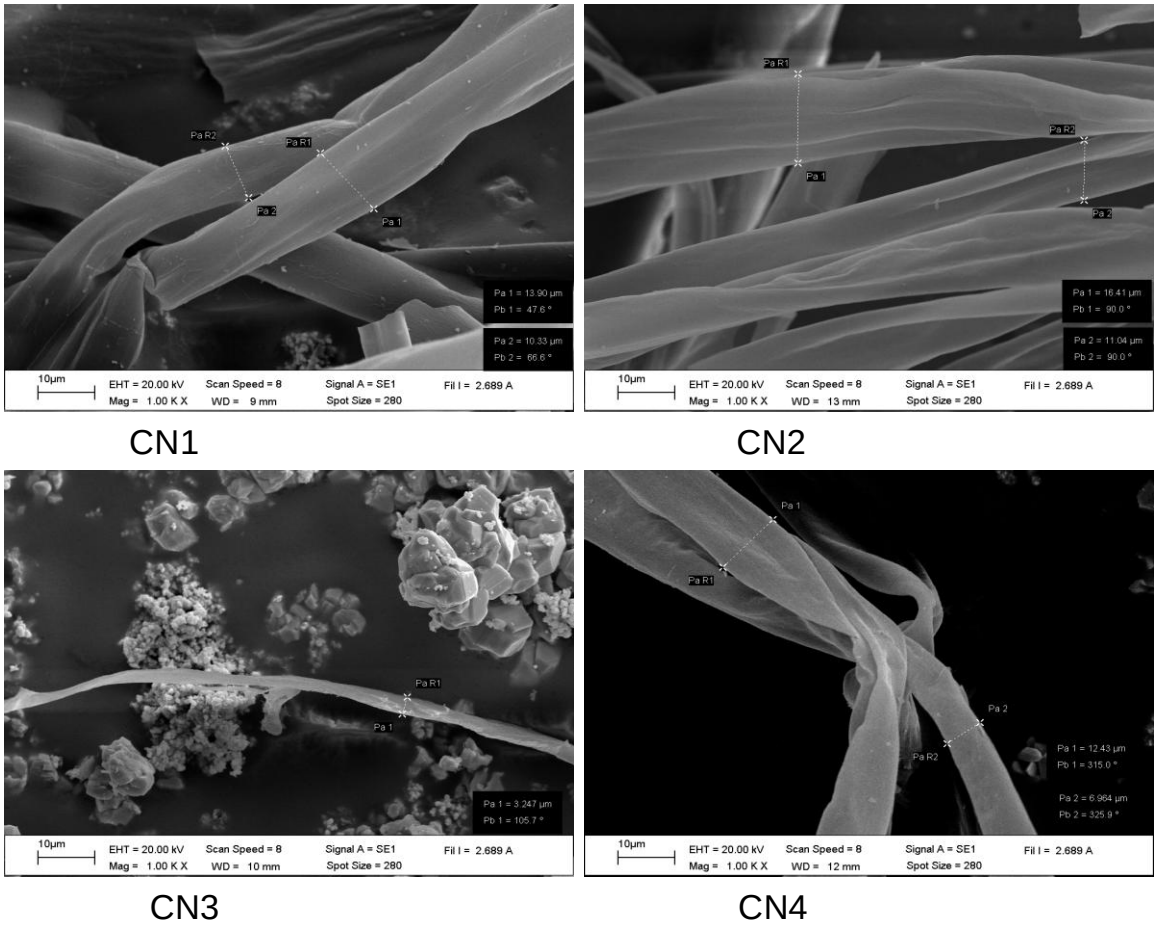

Figure 10. SEM micrographs of copper-kapok carbon fiber composites by pyrolysis at 400 to 700°C: CN1 = copper-kapok carbon fiber composite at 400°C, CN2 = copper-kapok carbon fiber composite at 500°C, CN3 = copper-kapok carbon fiber composite 600°C, and CN4 = copper-kapok carbon fiber composite at 700°C.

relatively smooth and has a peak at 1451 cm^{-1}. This shows that a number of functional groups have been broken up and carbon fibers are crystalline (Figure 3 MN4). The SEM images of composites at 700°C (Figure 11 MN4) have a large number of particles on the surface of carbon fiber. It is expected that the crystallization of Mg-C composite is formed, which corresponds to the results of XRD (Figure 7 MN4).

Figure 12 shows the surface of the zinc-kapok carbon fiber composites, it can be seen that the surface of carbon fiber is highly destroyed as compared to other composites, which is consistent with the results of XRD (Figure 8).

EDS analysis

Figure 13 shows the results of EDS comparison of the aluminium-carbon composites on surface of carbon fiber at 400 (Figure 13a) and 500°C (Figure 13b). The amount of C and Al increases, while the amount of O (derived from the Al_2O_3) decreases (Table 2), with increasing temperatures. It has been shown that Al can react with C in a greater proportion of the composite. It has resulted in reduced amounts of O as the temperature increased. It also shows that Al has been low oxidized to C. This results in a higher C content in the composite. In addition, Figure 9 AN1 and AN2 shows that the particles adhere on the surface of kapok carbon fiber at temperatures 500°C more than at 400°C. This result indicates that the composite is better formed at 500°C than at 400°C. The amount of Cu in Cu-kapok carbon fiber composite (pyrolysis at 400^{o}C) is up to 40.98% (Table 2) and C is oxidized to a large number. This is consistent with the percent yield (Table 1). It may be that the ratio of C in Cu-carbon composites is lower compared to Al-carbon composites. This phenomenon results in an increased amount of O in the composite. The XRD results obtained show that the composite has a higher crystallinity (Figure 6).

The magnesium-carbon fiber composite by pyrolysis at 400°C consists of 38.50 wt% C, 44.86 wt% O and 16.64

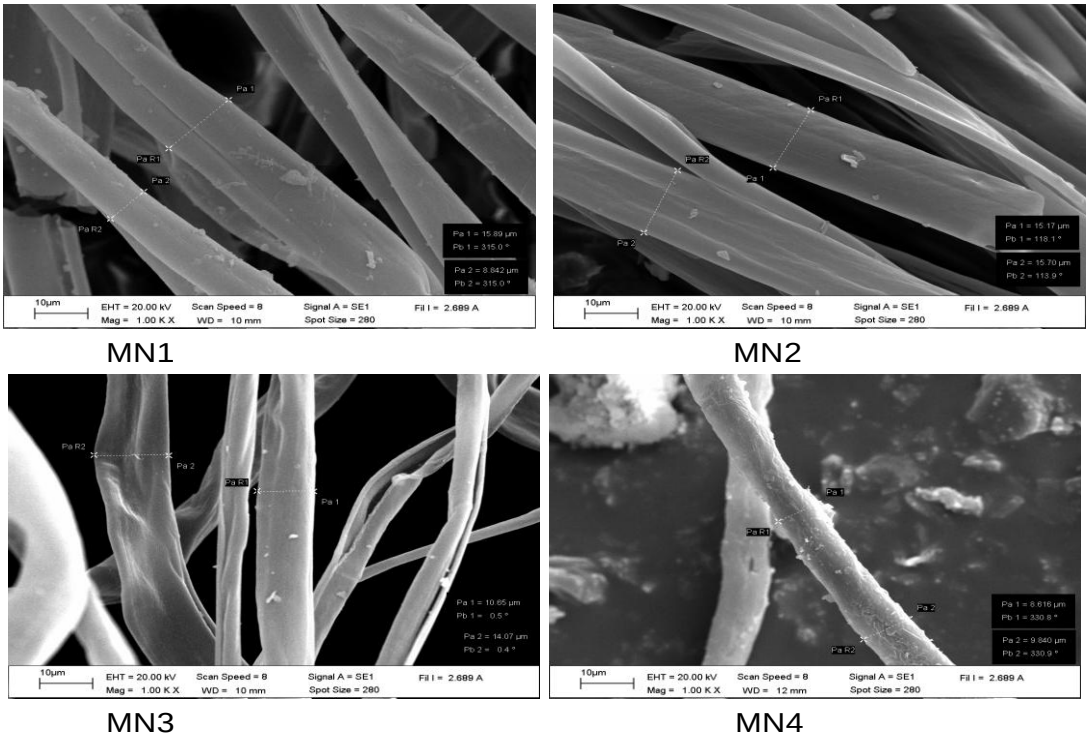

Figure 11. SEM micrographs of magnesium-kapok carbon fiber composites by pyrolysis at 400 to 700°C: MN1 = magnesium-kapok carbon fiber composite 400°C, MN2 = magnesium-kapok carbon fiber composite at 500°C, MN3 = magnesium-kapok carbon fiber composite at 600°C, and MN4 = magnesium-kapok carbon fiber composite at 700°C.

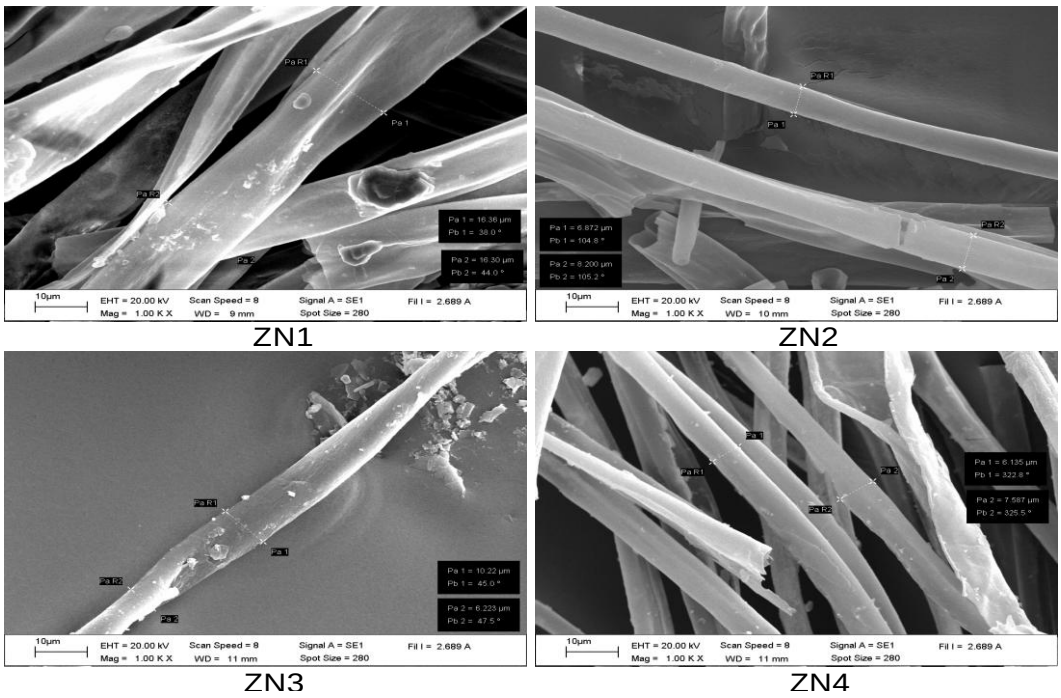

Figure 12. SEM micrographs of zinc-kapok carbon fiber composites by pyrolysis at 400 to 700°C: ZN1 = zinc-kapok carbon fiber composite at 400°C, ZN2 = zinc-kapok carbon fiber composite at 500°C, ZN3 = zinc-kapok carbon fiber composite at 600°C, and ZN4 = zinc-kapok carbon fiber composite at 700°C.

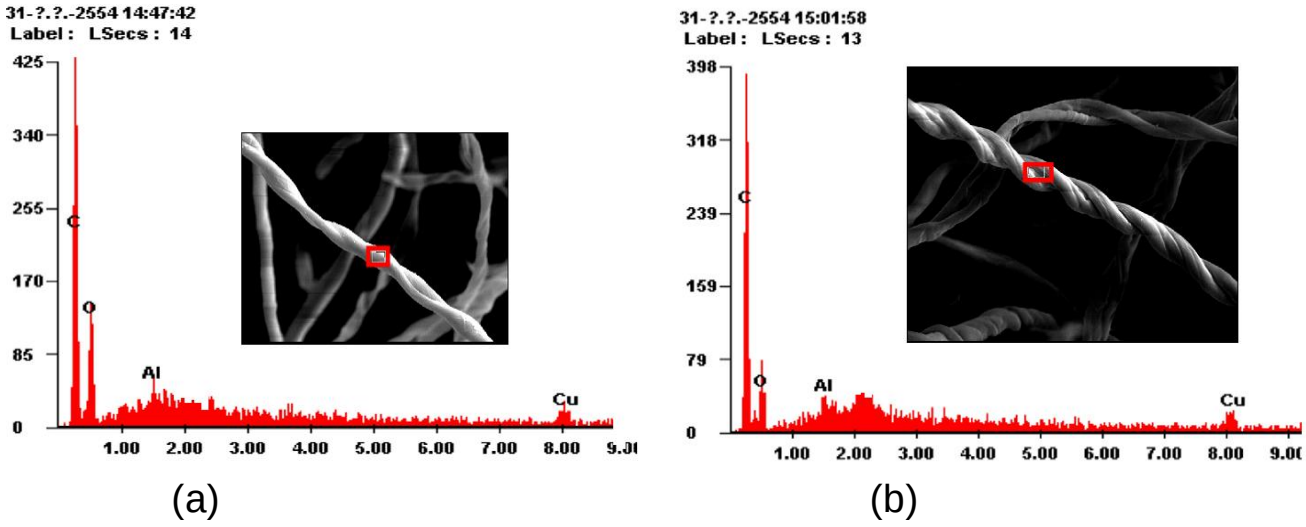

Figure 13. EDS spectrum of aluminium-carbon fiber composite by pyrolysis at 400°C (a) and 500°C (b).

Table 2. The composition of metals-carbon composites on surface of carbon fiber.

Composite type	Elements (wt%)						
	C	O	Al	Cu	Mg	Zn	Cl
Al-kapok carbon fiber composite -400°C	74.08	24.71	1.12	-	-	-	-
Al-kapok carbon fiber composite -500°C	82.50	16.21	1.29	-	-	-	-
Cu-kapok carbon fiber composite-400°C	38.60	20.40	-	40.98	-	-	-
Mg-kapok carbon fiber composite -400°C	38.50	44.86	-	-	16.64	-	-
Zn-kapok carbon fiber composite -400°C	8.33	6.36	-	-	-	44.10	41.17

wt% Mg (Table 2), which shows that the proportion of C that reacts with Mg and Cu is similar. However, in the case of Mg, $MgSO_4.7H_2O$ has been used as a catalyst. In the case of Cu, Cu $(NO_3)_2$ was used as a catalyst. It is expected that the kapok fiber to reacts more with oxygen in a $MgSO_4.7H_2O$ than with $Cu(NO_3)_2$. This results in higher oxygen in the Mg-C composite than Cu-C composite. Finally, the zinc-carbon fiber composite by pyrolysis at 400°C had the proportion of Zn and Cl higher than the proportion of C and O, which shows that Zn reacts quite well with Cl as compared with C. In addition, it has been found that Zn-carbon fiber composite has the lowest ratio of oxygen compared to other composites. This is because there is no O in the $ZnCl_2$ catalyst.

Conclusions

The percent yield of all composites have tendency decreased with increasing pyrolysis temperature. The FTIR and XRD spectra showed increasing of amorphous structure of all metals-composites as pyrolysis temperature increased. The peaks of OH stretching of all metals-composites are trend to narrowing with shifted to higher wavenumber as pyrolysis temperature increased. The intensity of peaks in FTIR spectra of all metals-composites is decreased with increasing of pyrolysis temperature. The SEM images showed that a large number of metals composite particles adhered on the surface of kapok carbon fiber. Of the percent yield, FTIR and SEM, it was found that the strength of the breakdown of kapok fiber metal salts are arranged in order Al_2O_3 < $ZnCl_2$ < $MgSO_4.7H_2O$ < $Cu(NO_3)_2$, which corresponds to the oxidizing strength of four metal salts. The amount of metal-carbon composite was ordered as follows: Zn-carbon composite < Cu-carbon composite < Mg-carbon composite < Al-carbon composite. Metals incorporated fibers are expected to possess larger hydrogen adsorption capacity than the fibers alone.

ACKNOWLEDGMENTS

This study was supported by Office of the Higher Education Commission, Ministry of Education, Thailand.

REFERENCES

American Standard of Testing Material (1994). Standard Test Method for Fixed Carbon in Activate Carbon ASTM D, pp. 3172-89.

American Standard of Testing Material (1996). Standard Test Method for Total Ash content of Activate Carbon ASTM D, pp. 2866-94.

American Standard of Testing Material (1996). Standard Test Method for Volatile Matter Content of Activate Carbon ASTM D, pp. 5832-95.

Birjega R, Vizireanu SI, Dinescu G, Nistor LC, Ganea R (2009). The effect of textural properties of the γ-Al_2O_3:Ni catalyst template on the nanostructured carbon grown by PECVD. Superlattice. Microst. 46(1-2): 97-301

Chena D, Chena L, Liua S, Mab CX, Chena DM, Wang LB (2004). Microstructure and hydrogen storage property of Mg/MWNTs composites. J. Alloy. Compd., 372: 231-237.

Chłopek J, Morawska-Chochół A, Paluszkiewicz C (2008). FTIR evaluation of PGLA – Carbon fibres composite behaviour under '*in vivo*' conditions. J. Mol. Struct., 875(1-3): 101-107.

Eswaramoorthi I, Sundaramurthy V, Dalai AK (2006). Partial oxidation of methanol for hydrogen production over carbon nanotubes supported Cu-Zn catalysts. Appl. Catal. A-Gen., 313(1): 22-34.

Fan H, Li Y, Sang S (2011). Microstructures and mechanical properties of Al_2O_3–C refractories with silicon additive using different carbon sources. Mater. Sci. Eng. A., 528(7-8): 3177-3185.

Fujii H, Ichikawa T (2006). Recent development on hydrogen storage materials composed of light elements. Physica B. 383: 45-48.

Huang ZG, Guo ZP, Calka A, Wexler D, Liu HK (2007). Effects of carbon black, graphite and carbon nanotube additives on hydrogen storage properties of magnesium. J. Alloy. Compd., 427: 94-100.

Imamura H, Tabata S, Shigetomi N, Takesue Y, Sakata Y (2002). Composites for hydrogen storage by mechanical grinding of graphite carbon and magnesium. J. Alloy. Compd., 330-332: 579-583.

Lim TT, Huang X (2007). Evaluation of hydrophobicity/oleophilicity of kapok and its performance in oily water filtration: Comparison of raw and solvent-treated fibers. Ind. Crop. Prod., 26: 125-134.

Ndungu P, Nechaev A, Khotseng L, Onyegebule N, Davids W, Mohammed R, Vaivars G, Bladegroen B, Linkov V (2008). Carbon nanomaterials synthesized using liquid petroleum gas: Analysis toward applications in hydrogen storage and production. Int. J. Hydrogen Energ., 33(12): 3102-3106.

Oh SY, Yoo DI, Shin Y, Seo G (2005). FTIR analysis of cellulose treated with sodium hydroxide and carbon dioxide. Carbohyd. Res., 340(3): 417-428.

Pamuła E, Błażewicz M, Paluszkiewicz C, Dobrzyński P (2001). FTIR study of degradation products of aliphatic polyesters–carbon fibres composites. J. Mol. Struct. 596(1-3): 69-75.

Paradise M, Goswami T (2007). Carbon nanotubes-Production and industrial applications. Mater. Design, 28: 1477-1489.

Park S-J, Seo M-K, Lee Y-S (2003). Surface characteristics of fluorine-modified PAN-based carbon fibers. Carbon, 41(4): 723-730.

Popov VN (2004). Carbon nanotubes: properties and application. Mater. Sci. Eng. R., 43: 61-102.

Rather S, Naik M, Hwang SW (2008). Room temperature hydrogen uptake of carbon nanotubes promoted by silver metal catalyst. J. Alloy. Compd., 475(1-2): L17-L21.

Schaller R, Maria D, Marques dos Santosa S, Tkalceca I, Carre˜no-Morelli E (2009). Investigation of hydrogen storage in carbon nanotube–magnesium matrix composites. Mater. Sci. Eng. A., 521-522: 147-150.

Wang R, Song D, Liu W, He X (2010). Effect of arc spraying power on the microstructure and mechanical properties of Zn–Al coating deposited onto carbon fiber reinforced epoxy composites. Appl. Surf. Sci., 257(1): 203-209.

Wu CZ, Wang P, Yaob X, Liua C, Chen DM, Lub GQ, Cheng HM (2006). Hydrogen storage properties of MgH_2/SWNT composite prepared by ball milling. J. Alloy. Compd., 420: 278-282.

Xu L, Song H, Chou L (2011). Carbon dioxide reforming of methane over ordered mesoporous NiO–MgO–Al_2O_3 composite oxides. Appl. Catal. B-Environ., 108-109: 177-190.